

Bone Mass Is Compromised by the Chemotherapeutic Trabectedin in Association With Effects on Osteoblasts and Macrophage Efferocytosis

Benjamin P Sinder,¹ Laura Zweifler,¹ Amy J Koh,¹ Megan N Michalski,¹ Lorenz C Hofbauer,² Jose Ignacio Aguirre,³ Hernan Roca,¹ and Laurie K McCauley^{1,4}

¹Department of Periodontics and Oral Medicine, University of Michigan School of Dentistry, Ann Arbor, MI, USA

²Center for Healthy Aging, Technische Universität Dresden Technical University Medical Center, Dresden, Germany

³Department of Physiological Sciences, College of Veterinary Medicine, University of Florida, FL, USA

⁴Department of Pathology, University of Michigan, Medical School, Ann Arbor, MI, USA

ABSTRACT

Macrophages have established roles supporting bone formation. Despite their professional phagocytic nature, the role of macrophage phagocytosis in bone homeostasis is not well understood. Interestingly, apoptosis is a pivotal feature of cellular regulation and the primary fate of osteoblasts is apoptosis. Efferocytosis (phagocytosis of apoptotic cells) is a key physiologic process for the homeostasis of many tissues, and is associated with expression of osteoinductive factors. To test effects of macrophage depletion and compromised phagocytosis on bone, 16-week-old male C57BL/6J mice were treated with trabectedin—a chemotherapeutic with established anti-macrophage effects. Trabectedin treatment reduced F4/80+ and CD68+ macrophages in the bone marrow as assessed by flow cytometry, osteal macrophages near the bone surface, and macrophage viability in vitro. Trabectedin treatment significantly reduced marrow gene expression of key phagocytic factors (*Mfge8*, *Mrc1*), and macrophages from treated mice had a reduced ability to phagocytose apoptotic mimicry beads. Macrophages cultured in vitro and treated with trabectedin displayed reduced efferocytosis of apoptotic osteoblasts. Moreover, efferocytosis increased macrophage osteoinductive TGF- β production and this increase was inhibited by trabectedin. Long-term (6-week) treatment of 16-week-old C57BL/6J mice with trabectedin significantly reduced trabecular BV/TV and cortical BMD. Although trabectedin reduced osteoclast numbers in vitro, osteoclast surface in vivo was not altered. Trabectedin treatment reduced serum P1NP as well as MS/BS and BFR/BS, and inhibited mineralization and *Runx2* gene expression of osteoblast cultures. Finally, intermittent PTH 1-34 (iPTH) treatment was administered in combination with trabectedin, and iPTH increased trabecular bone volume fraction (BV/TV) in trabectedin-treated mice. Collectively, the data support a model whereby trabectedin significantly reduces bone mass due to compromised macrophages and efferocytosis, but also due to direct effects on osteoblasts. This data has immediate clinical relevance in light of increasing use of trabectedin in oncology. © 2017 American Society for Bone and Mineral Research.

KEY WORDS: EFFEROCYTOSIS; MACROPHAGES; TRABECTEDIN; PARATHYROID HORMONE; OSTEOIMMUNOLOGY

Introduction

Bone not only provides a rigid structure enabling locomotion, but also houses critical physiologic functions such as hematopoiesis and supports the immune system. The environment of diverse cells in the bone marrow interact with their osteoblast and osteoclast neighbors on the bone surface, regulating bone homeostasis and structure. Myeloid cells are white blood cells that comprise a large portion (15% to 25%) of the marrow, and acquire defined roles regulating the development, homeostasis, and healing of many tissues. Investigating the role of myeloid cells in the bone marrow and specifically osteal macrophages in bone homeostasis was the focus of this study.

Despite the large number of macrophages in bone, their role supporting bone formation has only recently emerged.^(1,2) Evidence includes reports of depletion of a broad spectrum of monocyte and macrophage cells under the *csf1r* promoter leading to reduced osteoblast activity in vitro and in vivo, and significantly less bone mass.^(3,4) In addition, histologic studies identified a population of osteal macrophages (also known as OsteoMacs) that line a majority of bone formation surfaces in vivo,⁽³⁾ further linking bone resident macrophages to their support of bone formation. Interestingly, although macrophages (“big-eaters” in Greek) are literally named for their phagocytic ability, the professional phagocytic role of osteal macrophages in bone homeostasis has been largely overlooked.

Received in original form December 10, 2016; revised form June 7, 2017; accepted June 9, 2017. Accepted manuscript online June 10, 2017.

Address correspondence to: Laurie K McCauley, DDS, MS, PhD, University of Michigan School of Dentistry, 1011 N. University Ave., Ann Arbor, MI 48109, USA.

E-mail: mccauley@umich.edu

Additional Supporting Information may be found in the online version of this article.

Journal of Bone and Mineral Research, Vol. 32, No. 10, October 2017, pp 2116–2127

DOI: 10.1002/jbmr.3196

© 2017 American Society for Bone and Mineral Research

Macrophages eat a variety of targets including apoptotic cells. Given that the primary fate of osteoblasts is apoptosis^(5,6) and osteal macrophages are found intimately associated with osteoblast-lined bone surfaces,^(2,3) macrophages may support bone formation via their clearance of apoptotic bone cells. Yet the consequence of altered macrophage clearance of apoptotic osteoblasts is unclear.

Efferocytosis (phagocytosis of apoptotic cells) is an area of interest that has key physiologic roles in lung homeostasis,^(7,8) atherosclerosis,^(9,10) disease states such as systemic lupus erythematosus,⁽¹¹⁾ and cancer.⁽¹²⁾ In addition to clearing apoptotic cells and preventing buildup of a toxic microenvironment, efferocytosis also causes macrophage expression of specific chemoattractant and stimulatory cytokines such as TGF- β ^(13,14) and CCL-2.⁽¹⁵⁾ Recent data strongly suggests a role for efferocytosis in bone homeostasis. For example, although broad depletion of monocytes and macrophages decreased bone mass, an experimental model with increased phagocytic CD68+ cells had increased bone mass.⁽⁴⁾ In addition, increases in CD163+ cells and efferocytic gene expression (eg, MFG-E8, MRC1, ARG1) further suggested that changes in macrophage efferocytosis were related to the bone phenotype. However, efferocytosis was not directly assessed in that study. Therefore, the purpose of this study was to examine the role of macrophages and their efferocytic function in bone biology.

Specifically, we determined whether a model with decreased phagocytic CD68+ macrophages and reduced efferocytosis would result in low bone mass. In the present study, macrophages were manipulated via the chemotherapeutic agent trabectedin, which has been shown to selectively inhibit macrophages.⁽¹⁶⁾ There is also strong clinical motivation for this work. Although trabectedin was recently approved by the US Food and Drug Administration (FDA) for use in patients with soft-tissue sarcomas, and is presently in multiple clinical trials for additional forms of cancer,⁽¹⁷⁾ its impact on bone is unknown.

Materials and Methods

Animals

All animal experiments were performed with the approval of the University of Michigan Committee for the Use and Care of Animals. Skeletally mature 16-week-old C57BL/6J male mice (Jackson Laboratory, Bar Harbor, ME, USA) were used unless otherwise noted in long-term and short-term treatment regimens, housed three to five per cage in specific pathogen free (SPF) conditions, fed 5001 chow (Purina), randomized to groups, and given IDs for blinding during subsequent analyses. Trabectedin (Yondelis, PharmaMar, Madrid, Spain) was dissolved in dimethyl sulfoxide (DMSO) at a stock concentration of 1mM, and stored at -20°C until use. A long-term (6-week) treatment regimen was used where animals were administered trabectedin (0.15 mg/kg, i.v. tail vein, biweekly) or vehicle (0.9% saline and DMSO) under isoflurane. Trabectedin treatments were blinded to the injector. Because local tail vein injection site reactions can occur with trabectedin, 14 animals were allocated to the long-term trabectedin group, three of which were euthanized early due to local tail vein injection site reactions resulting in $n = 11/\text{group}$. A short-term treatment regimen (1 week) included a single injection of trabectedin (0.15 mg/kg, tail vein) or vehicle given at 16 weeks of age with $n = 8/\text{group}$. To assess the effect of anabolic intermittent parathyroid hormone 1-34 (iPTH) on macrophages and osteoblasts in conjunction with

trabectedin, mice were treated with iPTH (50 $\mu\text{g}/\text{kg}$ body weight, daily) or vehicle (0.9% saline [Veh]) with or without trabectedin (0.15 mg/kg, i.v. tail vein and retro-orbital, biweekly) for 6 weeks with $n = 10$ to 13/group. One Veh/iPTH mouse did not recover after isoflurane and vehicle i.v. injection, leaving Veh/Veh $n = 10$, Veh/iPTH $n = 9$, Trabectedin/Veh $n = 12$, Trabectedin/iPTH $n = 13$. Trabectedin treatment began 3 days prior to iPTH to ensure trabectedin effects at the onset of iPTH. For dynamic histomorphometry analysis, a cohort of animals ($n = 12/\text{group}$) were treated with trabectedin or vehicle (0.15 mg/kg), given calcein (30 mg/kg) injections 5 and 2 days before euthanasia, and euthanized 1 week after the single trabectedin injection.

Blood and serum ELISAs

Blood was harvested at euthanasia by intracardiac puncture, allowed to coagulate for several hours at room temperature, serum separated by centrifugation, stored at -80°C , and P1NP and tartrate-resistant acid phosphatase 5b (TRAcP5b) (Immunodiagnosics Systems, The Boldons, UK) were measured using enzyme immunoassays.

Flow cytometry

Marrow was flushed from the femur of mice immediately after euthanasia in FACS buffer (PBS with 2% FBS, 0.5mM EDTA). Each stain included 1×10^6 cells with anti-mouse F4/80 (BioLegend, San Diego, CA, USA, or Abcam, Cambridge, MA, USA; A3-1) or anti-mouse CD68 (BioLegend; FA-11). Isotype controls were used to confirm specificity. Flow cytometry was performed using a FACS ArialIII (BD Biosciences, San Jose, CA, USA).

Micro-computed tomography

Dissected and fixed (10% Neutral Buffered Formalin – NBF, 24hrs) tibiae were scanned by ex-vivo micro-computed tomography (μCT) at a 12- μm voxel size (Scanco μCT -100; Scanco Medical AG, Brüttisellen, Switzerland) and assessed following established guidelines.⁽¹⁸⁾ Trabecular bone parameters were measured over 40 slices (480 μm) immediately distal to the proximal growth plate by manually outlining the endocortical border and thresholding at 180 mg/cm^3 . Cortical bone parameters were measured over 30 slices (360 μm) extending distally from a location 3 mm proximal to the tibia-fibula junction. A threshold of 280 mg/cm^3 was used for cortical bone.

Histomorphometry and dynamic histomorphometry

Tibiae were fixed in 10% neutral buffered formalin (NBF), stored in 70% ETOH, decalcified in 14% ethylenediaminetetraacetic acid (EDTA), embedded in paraffin, and sectioned at 5 μm . A central slice of the proximal tibia was stained by H&E and bone morphometry was analyzed using OsteoMeasure software (OsteoMetrics, Decatur, GA, USA) and an Olympus (Tokyo, Japan) microscope for bone area/tissue area (BA/TA), Tb.Th, and Tb.N.^(19,20) The ROI began $\sim 200 \mu\text{m}$ distal to the proximal growth plate, extended 1215 μm distally, and was 1150 μm wide (or 50 μm from endocortical surface). An adjacent section was stained for tartrate resistant acid phosphatase (TRAP; Sigma, St. Louis, MO, USA; 387A) and hematoxylin. Using the ROI described above, osteoclast surface (Oc.S), bone surface (BS), and number of osteoclasts were quantified.⁽¹⁹⁾ Similarly, osteal macrophages were quantified by immunostaining of adjacent paraffin sections for F4/80 (Abcam; ab6640; Anti-Rat HRP-DAB

Kit; R&D Systems, Minneapolis, MN, USA) and identified by their proximity of within three cell diameters of the bone surface.⁽²¹⁾ Osteal macrophage number normalized to tissue area and bone surface were quantified. Dynamic histomorphometry was performed in 16-week-old C57BL/6J male mice treated with vehicle or trabectedin (0.15 mg/kg i.v., $n = 12$ /group) and given calcein injections 5 days and 2 days before euthanasia at 17 weeks of age. In brief, tibias were cut cross-sectionally, placed in 10% phosphate-buffered formalin for 48 hours, dehydrated in ethanol, and embedded undecalcified in methyl methacrylate. The proximal tibias were sectioned longitudinally at 8 μ m thicknesses with a Leica/Jung 2065 microtome and used to measure fluorochrome-based indices of bone formation. The ROI began 0.4 mm distal to the growth plate and excluded the primary spongiosa and cancellous bone within 0.1 mm of

the endocortical surfaces, including a 1.2 mm (width) by 3.6 mm (length) area. Mineral apposition rate (MAR), SL (Single Label), DL (Double Label), mineralizing surface (MS/BS), and bone formation rate per unit of bone surface (BFR/BS) were enumerated or calculated following recommendations of the Histomorphometry Nomenclature Committee of the American Society of Bone and Mineral Research.⁽²⁰⁾

RT-PCR

Bone marrow was flushed with TRIzol from the femur of mice treated with trabectedin or vehicle for 1 week, and RNA was isolated. For cell culture experiments, RNA was isolated with the RNeasy system (Qiagen, Valencia, CA, USA). In each case, RNA was quantified (Nanodrop, Thermo Fisher Scientific, Waltham,

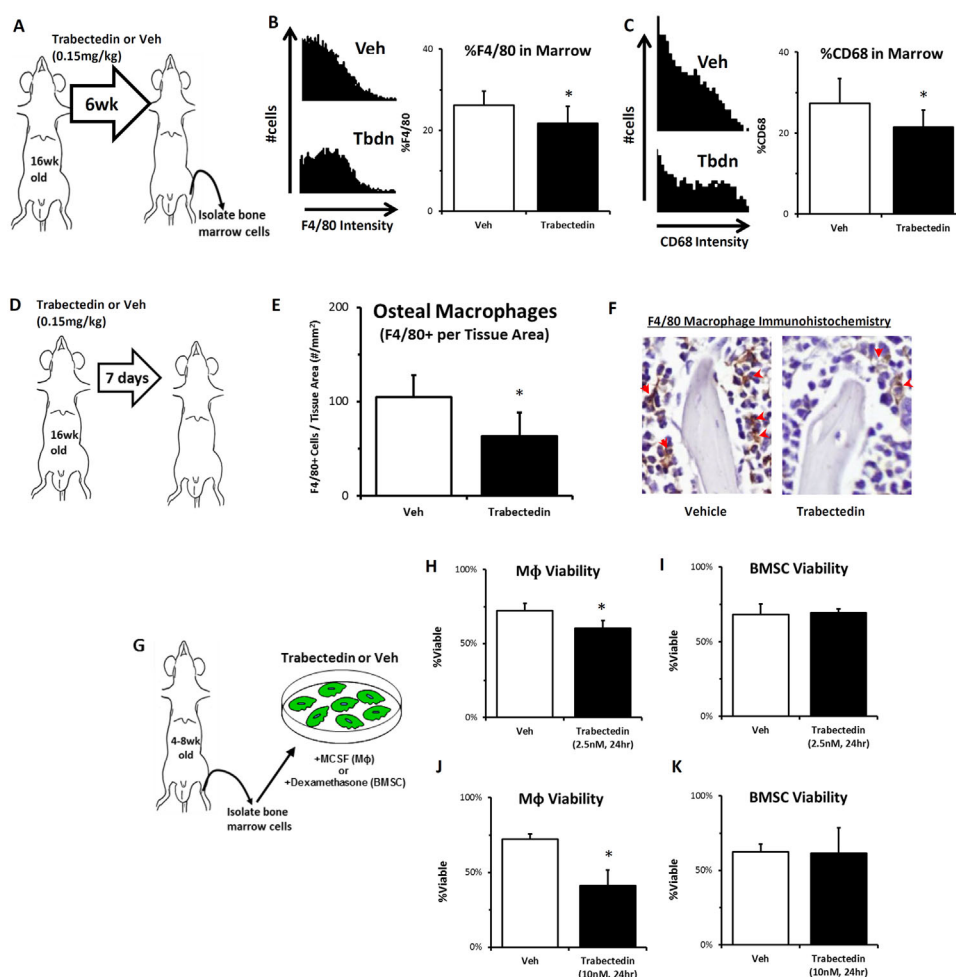


Fig. 1. Trabectedin treatment inhibits macrophages. (A) Male 16-week-old C57BL/6J mice treated with trabectedin (Tbdn) or vehicle (Veh) for 6 weeks (0.15 mg/kg, three biweekly injections, $n = 9$ to 13/group). After marrow extraction, cells were stained for F4/80 (B) and phagocytic marker CD68 (C), and analyzed by flow cytometry, with representative images shown. (D–F) In animals treated for 1 week with trabectedin, tibial paraffin sections of metaphyseal trabecular bone and stained for F4/80 by immunohistochemistry. Osteal macrophages per tissue area were quantified (E) and representative images are shown (F) with red arrows denoting examples of osteal macrophages (F4/80+ and within 3 cell diameters of bone surface). (G, H, J) To confirm a direct effect of trabectedin on macrophages, macrophages (M ϕ) were expanded from the bone marrow from 4-week-old to 8-week-old C57BL/6J mice with M-CSF, and viability assessed by trypan blue exclusion after trabectedin treatment. (G, I, K) Similarly, BMSCs from 4-week-old to 8-week-old C57BL/6J mice were expanded with dexamethasone, viability assessed after trabectedin treatment. Data are mean \pm SD. * $p < 0.05$ versus Veh. M ϕ = macrophages; Tbdn = trabectedin; Veh = vehicle.

MA, USA) and cDNA generated via reverse transcriptase reactions. cDNA products were amplified and detected with TaqMan Gene Expression PCR master mix (Applied Biosystems, Foster City, CA, USA) and TaqMan probes included *Mfge8* (Mm00500549_m1), *Mrc1* (Mm01329362_m1), *Mertk* (Mm00434920_m1), and *Runx2* (Mm00501584_m1). *Gapdh* (Mm99999915_g1) was used as the reference for bone marrow, and *Actb* (Mm02619580_g1) was used as a reference for in vitro experiments. Real-time PCR was analyzed on a ViiA7 (Applied Biosystems, Foster City, CA, USA) and quantified via the comparative threshold cycle ($\Delta\Delta Ct$) method.⁽²²⁾

Ex vivo phagocytosis assay

Bone marrow was flushed from the femur of mice 1 week after a single dose of trabectedin or vehicle and immediately co-cultured with FITC+ 5- μ m-diameter apoptotic-mimicry beads (Bangs Laboratories, Fishers, IN, USA) with a 1.1 ratio of cells: beads at 37°C (4°C was used as a control) in a flow cytometry tube. After 5 hours, cells were fixed with 1% formalin on ice for 1 hour, stained for F4/80 (APC), and analyzed by flow cytometry to assess phagocytosis. To visualize bead internalization and attachment to macrophages, samples were further analyzed using ImageStream (EMD Millipore, Billerica, MA, USA).

Efferocytosis of apoptotic osteoblasts in vitro

Primary macrophages were cultured by flushing bone marrow from the hindlimbs of 4-week-old to 8-week-old C57BL/6J with macrophage colony stimulating factor (M-CSF, 30 ng/mL; PeproTech, Rocky Hill, NJ, USA) for 1 week, and 750,000 cells were split into each well of a six-well plate as described.⁽¹⁵⁾ Macrophages attached overnight in α -MEM media with 5% FBS and 15 ng/mL M-CSF, and subsequently treated with 2.5nM trabectedin in DMSO or vehicle (DMSO) for 12 hours in low serum media (0.25% FBS). Prior to co-culture, osteoblastic MC4 (MC3T3-E1 subclone4)⁽²³⁾ cells were expanded, stained (DeepRed CellTracker; Thermo Fisher Scientific, Rockford, IL, USA), induced to apoptosis by 30 min of exposure to a UV light source (>90% Trypan Blue+), allowed to recover for 2 hours at 37°C, and added in equal number (1:1) to trabectedin-treated and vehicle-treated macrophages as described.⁽¹⁵⁾ After 1 hour, the efferocytic co-culture was stopped by fixation with 1% formalin, cells were harvested, and macrophages were stained green (FITC, F4/80). Efferocytosis was assessed as the percentage of double positive FITC macrophages and Deep Red-stained apoptotic MC4 cells by flow cytometry.

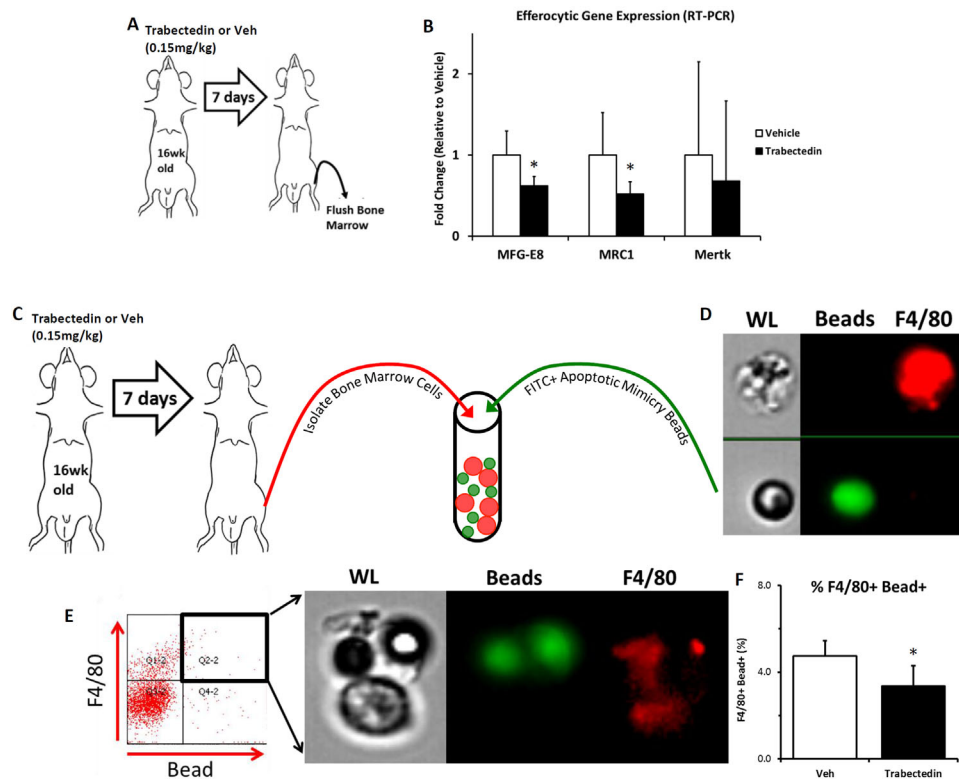


Fig. 2. In vivo trabectedin treatment reduces phagocytic ability of macrophages. (A) Sixteen-week-old male C57BL/6J mice were treated for 1 week with trabectedin (0.15 mg/kg) or vehicle (Veh). Marrow was extracted and mRNA isolated to assess gene expression. (B) Significantly decreased expression of *Mfge8* (linker protein that facilitates efferocytosis) and *Mrc1* (marker of alternatively activated efferocytic macrophages), and unaltered levels of *Mertk* (protein that facilitates efferocytosis). (C) Fresh bone marrow cells were isolated from 16-week-old male C57BL/6J mice treated for 1 week with trabectedin (0.15 mg/kg) or Veh, and immediately co-cultured with FITC+ apoptotic mimicry beads. After 5 hours of phagocytosis, co-cultures were fixed, macrophages were stained for F4/80 (D), and the percent of F4/80+ macrophages that ingested or were attached to a FITC+ bead was assessed via flow cytometry (E). Trabectedin significantly reduced phagocytosis within the F4/80 macrophage population (F). $n = 8$ /group. Data are mean \pm SD. * $p < 0.05$ versus Veh. Veh = vehicle; WL = White Light.

TGF- β secretion by efferocytic macrophages

Macrophages treated with vehicle or trabectedin were co-cultured with apoptotic MC4 cells as described in previous methods section. After 18 hours of co-culture, supernatants were harvested to assess secreted TGF- β by macrophages in response to efferocytosis. Supernatants were exposed to acid to convert to active TGF- β , and then active TGF- β was assessed with a commercially available ELISA (R&D Systems). The α -MEM media supplemented with 0.25% FBS contained undetectable levels of TGF- β (data not shown).

Viability of macrophages, MC4 cells, calvarial osteoblasts, and bone marrow stromal cells

Macrophages from 4-week-old to 8-week-old C57BL/6J mice were expanded with M-CSF and plated at 750,000 per well in six-well tissue culture plates as described in previous "Efferocytosis of apoptotic osteoblasts in vitro" methods section. MC4 cells, and bone marrow stromal cells (BMSCs) isolated from 4-week-old to 8-week-old C57BL/6J mice and expanded with 10nM

dexamethasone, were cultured as described. Primary calvarial osteoblasts were isolated from 4-day-old to 10-day-old C57BL/6J mice per published protocols.⁽²⁴⁾ BMSCs, MC4 cells, and macrophages were treated with vehicle (DMSO) or trabectedin. Cells were removed from the plate with 0.25% trypsin immediately after treatment, or after being returned to normal α -MEM with 10% FBS for 4 days, and viability and cell number were assessed by trypan blue staining with a hemocytometer.

Osteoclast formation and resorption assays

Marrow was flushed from the long bones of 4-week-old to 8-week-old C57BL/6J mice into a 100-mm dish in α -MEM with 10% FBS and 1% penicillin-streptomycin-glutamine (PSG) overnight. The next day, suspension cells were re-plated in new 100-mm Petri culture plastic dishes with 30 ng/mL of M-CSF, and expanded for 4 to 5 days until confluent. Cells were then split with ice-cold PBS containing 1 μ M EDTA and re-plated at 60,000/cm² in 48-well or 96-well plates with 30 ng/mL of M-CSF and 50 ng/mL of murine RANKL (PeproTech, Rocky Hill,

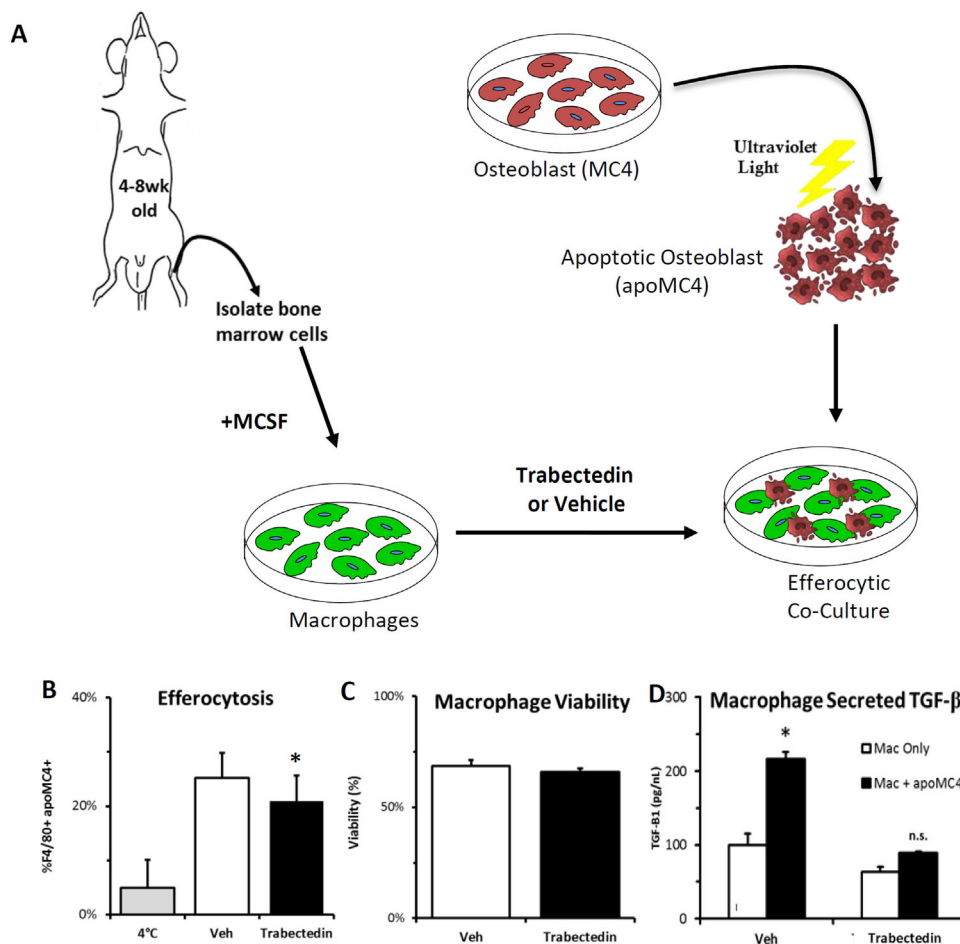


Fig. 3. Reduced macrophage efferocytosis with trabectedin in vitro. (A) Marrow was extracted from 4-week-old to 8-week-old C57BL/6J mice, and macrophages expanded with M-CSF for 1 week. MC4 cells were stained red via DeepRedCell tracker dye, induced to apoptosis by UV light, and subsequently added to macrophages that were treated with trabectedin or vehicle. Macrophages were subsequently stained for F4/80 with a FITC fluorophore. (B) Efferocytosis was assessed by double-positive F4/80 and apoptotic MC4 cells, and efferocytosis was reduced by trabectedin pretreatment at a dose (2.5nM, 12 hours) that did not affect (C) macrophage viability ($n = 6$ to 9/group). (D) Macrophages secreted significantly more osteoinductive TGF- β with efferocytosis, and this increase was inhibited by trabectedin (10nM, 24 hours) in vitro as assessed by ELISA ($n = 3$ /group). Data are mean \pm SD. * $p < 0.05$ versus Veh. Veh = vehicle.

NJ, USA). Once multinucleated osteoclasts began forming (4 to 5 days), wells were treated with trabectedin or vehicle. Cells were subsequently fixed with 10% formalin, stained for TRAP (Sigma, St. Louis, MO, USA; 387A), and enumerated. To assess effects of trabectedin on resorption, similar experiments were carried out on 96-well Corning Osteo Assay plates (Sigma, St. Louis, MO, USA) coated with hydroxyapatite, and hydroxyapatite dissolution was assessed. Macrophages were first grown as described above in separate plates with M-CSF and then similarly split in equal number into wells of Corning Osteo Assay plates and RANKL added. After osteoclastogenesis on D3-D4 in the Corning Osteo Assay plate, cells were treated with trabectedin at specified doses, replaced with normal osteoclast media for an additional 24 hours after treatment, and resorption area was quantified as the percent of white area.

Osteoblast mineralization and gene expression

Primary calvarial osteoblasts were isolated from 4-day-old to 10-day-old C57BL/6J mice per published protocols,⁽²⁴⁾ and cultured in α -MEM with 10% FBS and 1% PSG. Once cells reached confluence (day 0), media was supplemented with 50 μ M ascorbic acid for gene expression or 50 μ M ascorbic acid plus 10mM β -glycerol phosphate for mineralization assays with every media change. MC4 cells were grown under identical conditions. Osteoblasts used for gene expression were treated from day 4 to

day 5 with varying doses of trabectedin and RNA was collected on day 5. Osteoblasts assayed for mineralization were similarly treated from day 4 to day 5, subsequently replaced with media supplanted with 50 μ M ascorbic acid plus 10mM β -glycerol phosphate and allowed to mineralize to day 14 (MC4) or day 21 (calvarial osteoblasts). Von Kossa staining was performed as described.⁽²⁵⁾

Statistical analysis

Student's *t* test, or paired *t* test, was used where appropriate and after normality was assessed. The trabectedin and iPTH in vivo data with 2×2 experimental design was analyzed by two-way ANOVA, and least significant difference (LSD) post hoc test. Power analysis calculations assuming 5% type I error indicated that $n=8$ /group had a 85% chance to detect a difference between means based on 1.5 standard deviations between groups—assumptions based on historical data. Values of $p < 0.05$ were considered significant, and data are shown as mean \pm SD.

Results

Trabectedin inhibits macrophages and phagocytic cells in vivo and in vitro

Trabectedin treatment in vivo reduced F4/80+ macrophages in the bone marrow by 16% compared to vehicle when assessed after 6 weeks of treatment (Fig. 1A, B). In addition,

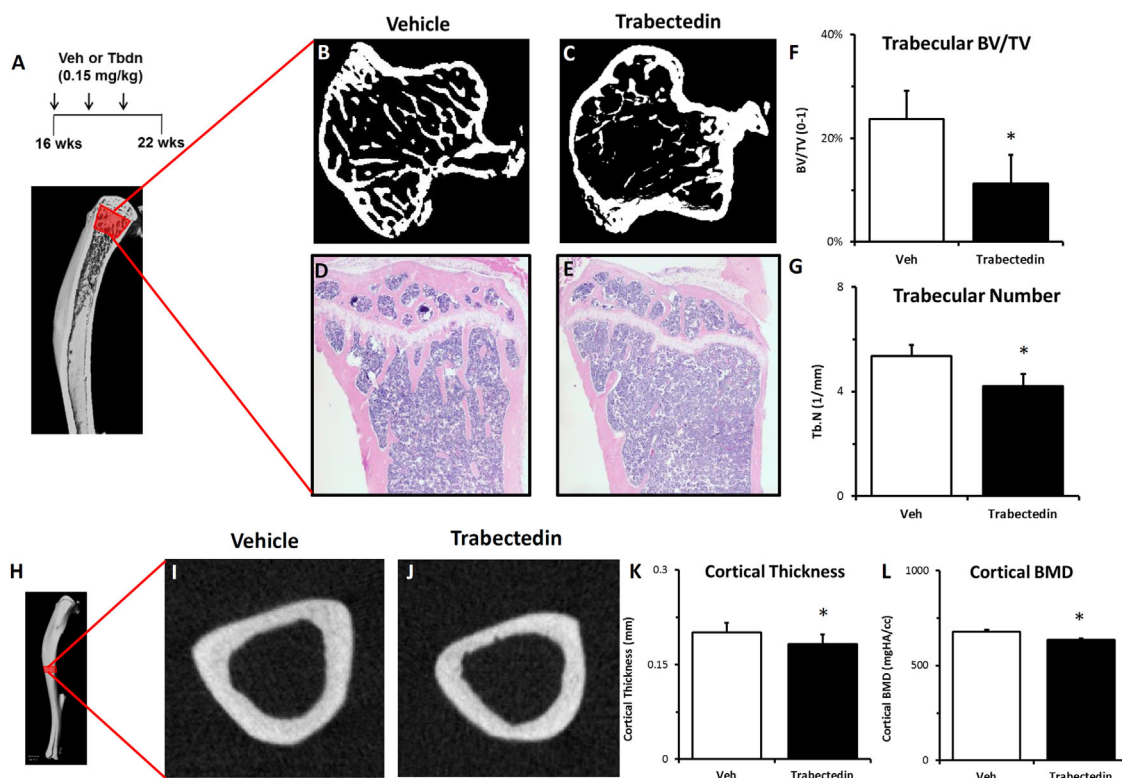


Fig. 4. Trabectedin reduces trabecular and cortical bone properties. (A) Long-term treatment regimen (6 weeks, 0.15 mg/kg, 3 \times) with trabectedin (Tbdn) or vehicle (Veh) was used to assess whole-bone changes the proximal tibia of 16-week-old male C57BL/6J mice. (B–E) Representative μ CT and H&E images show reduced trabecular bone mass with treatment. (F, G) Quantification of μ CT revealed a decrease in trabecular BV/TV due to significantly reduced trabecular number. (H) Trabectedin effects were also assessed in cortical bone of the diaphyseal tibia. (I, J) Representative μ CT images show decreased cortical bone, including reduced cortical thickness (K) and BMD (L). $n=11$ /group. Data are mean \pm SD. * $p < 0.05$ versus Veh. Tbdn = trabectedin; Veh = vehicle.

phagocytic CD68+ cells in the bone marrow were reduced by 23% with trabectedin treatment (Fig. 1C). Osteal macrophages, identified as F4/80+ cells near the bone surface, were significantly reduced (~39%) per tissue area (Fig. 1D–F) as well as per bone surface (data not shown). In vitro experiments confirmed trabectedin directly inhibits macrophages. Primary murine macrophages grown with M-CSF for 1 week were treated with trabectedin and viability

assessed by trypan blue exclusion. Treatment for 24 hours with 10nM trabectedin significantly decreased macrophage viability by 43%, and 24 hours with 2.5nM trabectedin decreased macrophage viability by 17% (Fig. 1G, H, J). BMSCs expanded from marrow with dexamethasone were treated with identical doses of trabectedin and no significant difference in viability was observed (Fig. 1I, K), indicating relative specificity to the myeloid lineage.

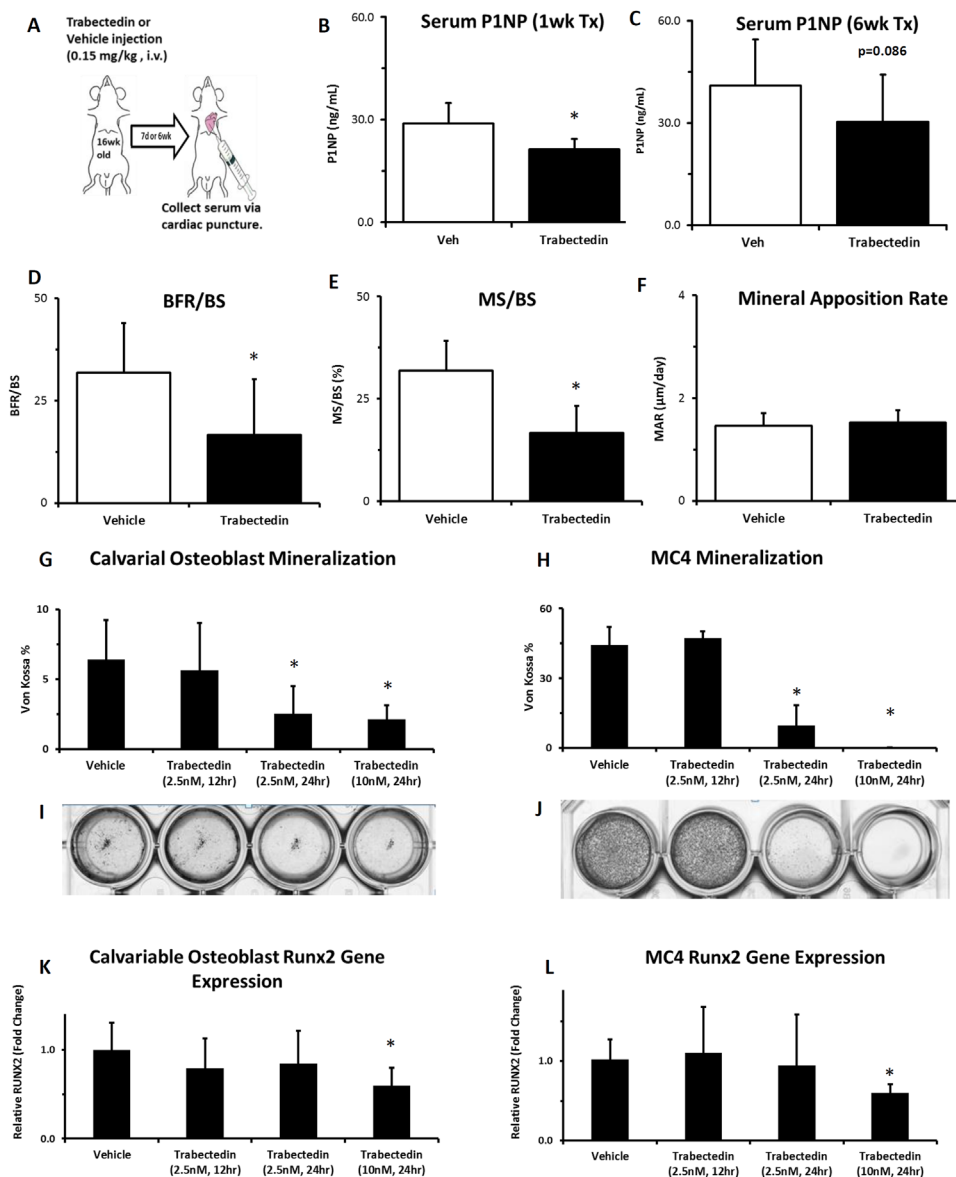


Fig. 5. Trabectedin reduces markers for bone formation and mineralization. (A) Short-term (1 week, single injection 0.15 mg/kg, $n = 8$ /group) or long-term (6 weeks, 3 biweekly injections, 0.15 mg/kg, $n = 11$ /group) with trabectedin or vehicle (Veh) reduced serum P1NP, a marker of bone formation. (D–F) A cohort ($n = 12$ /group) of mice were treated with trabectedin or vehicle for 1 week as shown in A and given calcein injections 5 or 2 days prior to euthanasia to facilitate dynamic histomorphometric analysis of tibial trabecular bone. Trabectedin treatment significantly reduced BFR/BS and MS/BS, but not MAR. (G, I) To assess direct effects of trabectedin on osteoblasts, calvarial osteoblasts were isolated from 4-day-old to 10-day-old C57BL/6J mice and treated with trabectedin from days 4 to 5, replaced with normal mineralization media with ascorbic acid and beta-glycerophosphate until day 21, and stained for Von Kossa ($n = 6$ /group). Representative images are shown. (H, J) The same treatment strategy as in G, I was used in the MC4 cell line, and stained via Von Kossa at day 14 ($n = 6$ /group). (K, L) To assess effects of trabectedin on osteoblast gene expression, both calvarial osteoblasts and MC4 cells were treated with trabectedin from days 4 to 5 and assessed by RT-PCR for relative *Runx2* expression ($n = 6$ /group). * $p < 0.05$ relative to Veh. Data are mean \pm SD. Tx = treatment; Veh = vehicle.

Trabectedin leads to reduced efferocytic gene expression and reduced macrophage efferocytosis

One week after a single injection of trabectedin, total gene expression in the marrow showed reduced levels of key macrophage efferocytosis mediators *Mfge8* (–48%) and *Mrc1* (–38%) (Fig. 2A, B). To assess functional changes in phagocytosis, marrows harvested from mice 1 week after a single injection of trabectedin were immediately co-cultured with FITC+ apoptotic mimicry beads. The co-culture was stained for F4/80 and flow cytometry analysis revealed a significant decrease (–28%) in phagocytosis as indicated by the %F4/80+Bead+ cells (Fig. 2C–F). In vitro experiments extended this finding using apoptotic osteoblasts as the prey. Apoptotic osteoblastic MC4 cells were added in co-culture to primary macrophages that were treated with trabectedin. Trabectedin treatment of macrophages reduced their efferocytosis of apoptotic MC4 osteoblasts as indicated by significantly reduced double-positive (%F4/80+ apMC4+) cells without significant compromise in viability (Fig. 3A–C). Macrophage efferocytosis significantly increased secretion of

osteoinductive TGF- β , and this increase was inhibited by trabectedin in vitro (Fig. 3D).

Trabectedin significantly reduces trabecular and cortical bone mass

The bone phenotype was evaluated in mice treated with trabectedin for 6 weeks (three biweekly administrations). In the proximal tibia, BV/TV was significantly reduced (–52%) compared to vehicle controls as measured by μ CT (Fig. 4A–F). Reductions in BV/TV were the result of large decreases in Tb.N (–21%) (Fig. 4G) and increases in Tb.Sp but no significant change in Tb.Th (data not shown). Histologic evaluation of the proximal tibia on H&E-stained sections (Fig. 4D, E) confirmed the μ CT data, and showed an 84% reduction in BA/TA (data not shown). In cortical bone of the diaphyseal tibia, similar findings of decreased bone mass were observed, evidenced by reduced cortical thickness (–9%) and cortical BMD (–6%) (Fig. 4H–L). Ct.Ar/Tt.Ar was significantly reduced (–7%), Ct.Ar trended less (–9%, $p = 0.06$), and Tt.Ar was unchanged ($p = 0.72$) (data not shown).

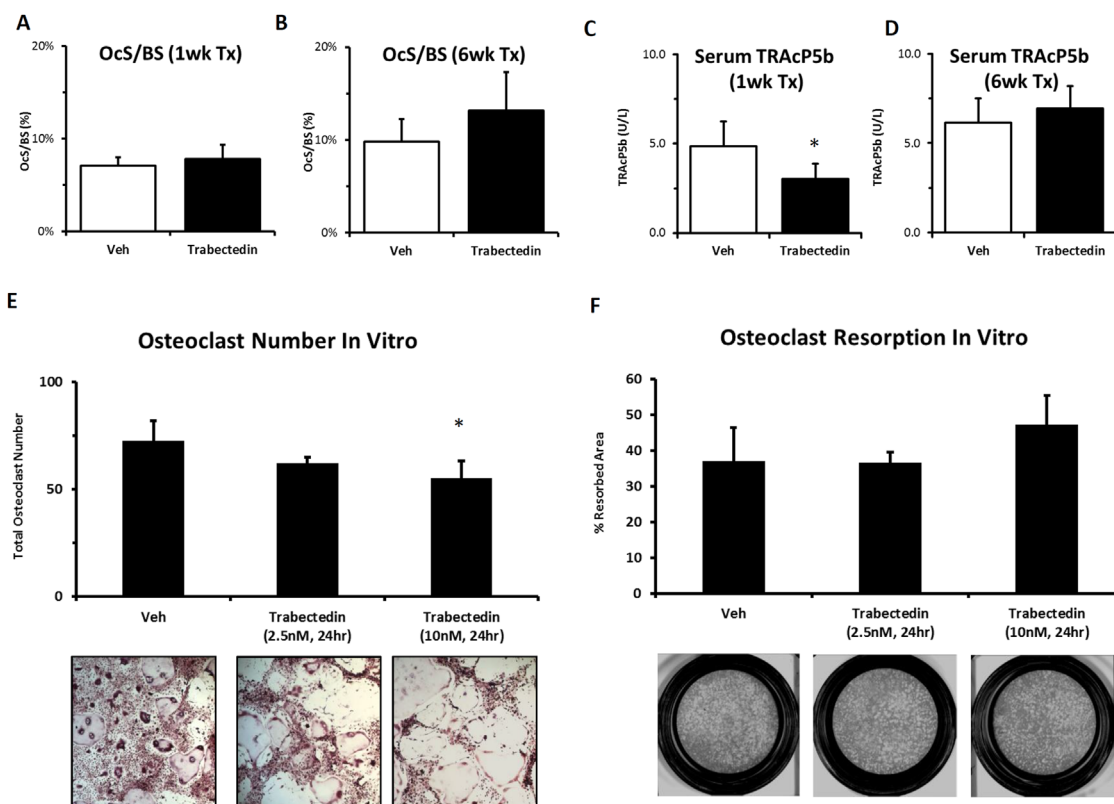


Fig. 6. Analysis of trabectedin effects on osteoclasts. (A,B) Both short-term (1 week, single injection 0.15 mg/kg, $n = 8$ /group) or long-term (6 weeks, 3 biweekly injections 0.15mg/kg, $n = 11$ /group) trabectedin treatment regimens were performed and OcS/BS was assessed by TRAP staining of a central slice of the proximal tibia. (C, D) In these same mice, serum TRAcP5b was quantified. (E) To assess direct effects of trabectedin on osteoclast number in vitro, osteoclasts were cultured from the marrow of 4-week-old to 8-week-old C57BL/6J mice with M-CSF and RANKL. After osteoclastogenesis on days 4 to 5, cells were treated with trabectedin at specified doses, stained for TRAP, and enumerated ($n = 6$ /group). Representative images are shown beneath. (F) To assess functional changes in resorption with trabectedin, osteoclasts were grown on Corning Osteo Assay plates under identical conditions, treated with trabectedin on days 4 to 5, replaced with normal osteoclast media for an additional 24 hours after treatment, and resorption area was quantified as the percent of white area. Representative images are shown. * $p < 0.05$ relative to Veh. Data are mean \pm SD. Veh = vehicle; OcS/BS = osteoclast surface per bone surface.

Trabectedin reduces bone formation, and directly inhibits osteoblast gene expression and mineralization in vitro

Serum P1NP, a marker of bone formation, was significantly decreased (−27%) 1 week after a single trabectedin injection, and trended toward a decrease (−26%, $p = 0.086$) after 6 weeks of trabectedin treatment (Fig. 5A–C). Dynamic histomorphometry of tibial trabecular bone 1 week after a single injection of trabectedin showed significantly reduced MS/BS (−42%) and BFR/BS (−48%) (Fig. 5D, E). The remaining areas of dual label after trabectedin treatment showed no significant change in MAR relative to vehicle (Fig. 5D–F). To determine if reductions in bone formation were related to direct effects of trabectedin on osteoblastic cells, osteoblast in vitro assays were performed. Primary calvarial osteoblasts were cultured in mineralization media, and treated with trabectedin from day 4 to day 5, and subsequently allowed to mineralize in trabectedin-free mineralization media to day 21. At day 21, Von Kossa staining revealed significantly less mineralization in calvarial osteoblasts treated with trabectedin (Fig. 5G, I). *Runx2* gene expression was also reduced in primary calvarial osteoblast cells using the same treatment strategy and assessing acute gene expression on day 5 in the highest trabectedin dose (Fig. 5K). Both of these findings in primary calvarial osteoblasts were corroborated by parallel experiments performed in the MC4 cell line (Fig. 5H, J, L). In MC4 cells, *Runx2* gene expression was significantly reduced at day 5 (Fig. 5I), and mineralization was significantly lower at day 14 with trabectedin treatment (Fig. 5E, G). Using an identical treatment protocol in both calvarial and MC4 osteoblasts, but assessing cell viability, it was found that after 24 hours treatment did not significantly impact osteoblast viability (Supporting Fig. 1A). However, treatment for 24 hours, and then replacement with normal media for 4 additional days led to significantly compromised osteoblast cell number by day 5 (Supporting Fig. 1B).

Trabectedin effects on osteoclasts

Histologic osteoclast analysis by TRAP staining in sections of the proximal tibia revealed no change in Oc.S/BS 1 week after a single injection of trabectedin, or after 6 weeks of biweekly treatment (Fig. 6A, B). Similar histologic TRAP staining data was observed for N.Oc/BS (data not shown). Serum analysis of TRAcP5b showed no change after 6 weeks of treatment, but did show a significant decrease 1 week after a single injection (−38%) (Fig. 6C, D). To assess direct effects of trabectedin on osteoclasts, primary murine osteoclasts were differentiated with RANKL and treated with trabectedin. After cells differentiated into osteoclasts on approximately day 4 of culture, trabectedin treatment decreased the total number of multinucleated TRAP⁺ cells by 24% (Fig. 6E). Detailed analysis revealed that while trabectedin decreased the number of smaller osteoclasts with dense cytoplasm, large osteoclasts were similar in number with treatment but appeared to have less dense cytoplasm with trabectedin treatment. To assess functional effects of trabectedin on bone resorption in vitro, osteoclasts were cultured on hydroxyapatite coated plates. After osteoclasts began to form on approximately day 4 of culture, wells were treated with trabectedin for 24 hours, subsequently replaced with normal osteoclast media for 24 additional hours, and assessed for resorption pits. No significant change in resorption pit area was detected with trabectedin treatment (Fig. 6F).

Anabolic PTH treatment in combination with trabectedin

Anabolic treatment with intermittent PTH 1-34 (iPTH) significantly increased tibial trabecular BV/TV due to increases in Tb.N in non-trabectedin-treated mice (Fig. 7A–C). Similar to Fig. 4, 6 weeks of trabectedin treatment reduced trabecular BV/TV due to a reduction in Tb.N. iPTH treatment significantly increased BV/TV in trabectedin-treated mice due to significant changes in Tb.N. However, Tb.N in mice treated with both iPTH and trabectedin was significantly less than untreated Veh/Veh controls (Fig. 7C). BV/TV in mice receiving both trabectedin and iPTH was not significantly different than untreated control mice.

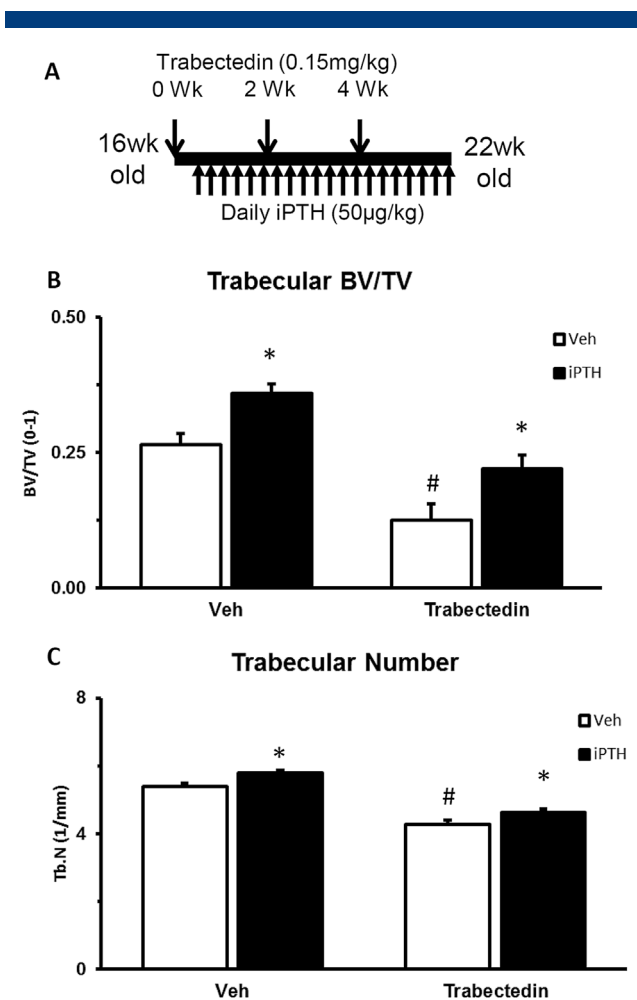


Fig. 7. Anabolic PTH partially rescues trabectedin treatment effects. (A) Male 16-week-old C57BL/6J mice were treated in a 2 × 2 study design for 6 weeks with either trabectedin or its vehicle control, and/or intermittent PTH 1-34 (iPTH) or its vehicle control ($n = 9$ to 13/group). To ensure trabectedin was having biologic activity at the commencement of anabolic therapy, iPTH was started 3 days after the first trabectedin injection. (B) Trabectedin significantly reduced trabecular tibial BV/TV, iPTH increased BV/TV, and iPTH was able to increase BV/TV in trabectedin treated mice. (C) Changes in BV/TV were largely due to changes in Tb.N. On an absolute level, untreated vehicle control mice had a greater Tb.N than mice treated with both trabectedin and iPTH, suggesting iPTH did not completely rescue the trabectedin phenotype. * $p < 0.05$ versus respective vehicle. # $p < 0.05$ versus vehicle/vehicle. Data are mean ± SD. Veh = vehicle.

Discussion

This study focused on macrophage contributions to skeletal homeostasis and adds new data to the field of osteoimmunology. Although significant contributions have been made that show the effect of macrophage number on bone, data in this study extends the field by examining functional changes in macrophage efferocytosis, thereby highlighting a new mechanism by which macrophages impact bone mass. The results also have immediate clinical relevance as trabectedin is currently administered to patients for the treatment of cancer,⁽¹⁷⁾ with no information about the impact on the skeleton. Thus, the data presented in this study has immediate implications for patients receiving trabectedin treatment.

The results of this study add to a growing body of literature highlighting the impact of osteal macrophages on bone formation and bone mass. Previously, data found an association between elevated phagocytic CD68+ cells, increased levels of efferocytic genes, and increased bone mass.⁽⁴⁾ Because efferocytosis was not directly assessed, a central purpose of the present study was to determine whether a model with reduced CD68+ cells and efferocytosis would have an associated decrease in bone mass. Indeed, trabectedin treatment in mice reduced phagocytic CD68+ macrophages and decreased bone mass. Importantly, we extended the investigation of decreased efferocytic gene expression and directly assayed changes in phagocytosis and efferocytosis with trabectedin. Data show that F4/80+ cells were less able to phagocytose apoptotic mimicry beads, suggesting that the macrophages were not only fewer in number but also less functional. This data was corroborated by *in vitro* studies showing that trabectedin-treated macrophages were less able to phagocytose apoptotic osteoblasts. Of note, macrophages efferocytosing apoptotic osteoblasts secreted significantly more TGF- β , a well-characterized osteoinductive factor, suggesting a functional consequence of efferocytosis. This increase was inhibited by macrophage pretreatment with trabectedin. We note that our data do not prove that efferocytosis and macrophage-derived TGF- β are responsible for bone forming effects, and it may be that apoptotic cell clearance itself is responsible for a positive impact of macrophage efferocytosis on bone. Collectively, these data supports a model whereby macrophages promote bone homeostasis in part by their efferocytic function.

In addition to effects on macrophages, we also observed effects of trabectedin on bone formation *in vivo* as well as direct effects on osteoblasts *in vitro*. The *in vivo* serum marker of bone formation, P1NP, showed reduced levels with trabectedin treatment. Similarly, dynamic histomorphometry of metaphyseal tibial trabecular bone also showed reduced bone formation as evidenced by significantly lower MS/BS and BFR/BS with trabectedin treatment. One possibility to explain reduced serum P1NP and bone formation *in vivo* is that it is an indirect effect of inhibiting macrophages^(4,26) and compromising efferocytosis. However, to determine if trabectedin may also have a direct effect on osteoblasts, we treated primary calvarial, and MC4 osteoblasts *in vitro* with trabectedin. Our data showed that trabectedin inhibited mineralization of both calvarial osteoblasts, and MC3T3 (subclone 4) cells *in vitro*. Moreover, this inhibition of mineralization was corroborated by reduced *Runx2* gene expression in both osteoblast cell types. Although this data demonstrates a direct effect of trabectedin on osteoblasts, the mechanism underlying the data is unclear. We note that

mineralization effects on trabectedin are greater in magnitude than effects on *Runx2*, suggesting that mineralization effects may also be due to general toxicity to osteoblasts (Supporting Fig. 1). Trabectedin interacts with TNF-related apoptosis-inducing ligand (TRAIL), which mediates its monocytic cell inhibition. TRAIL receptors are present on osteoblasts, and may regulate cell death under certain conditions.^(27–29) Other possibilities include that trabectedin can bind to the DNA minor groove and inhibit FUS/CHOP (Fused in Sarcoma/C/EBP homologous protein) fusion proteins that support osteoblasts,^(30,31) and cells deficient in homologous recombination are particularly sensitive to trabectedin effects. Regardless of the mechanism, trabectedin did appear to directly influence osteoblasts, even though its effect on cell viability was greater in macrophages than BSMCs.

Trabectedin effects on osteoclasts were more varied. Trabectedin treatment of osteoclasts *in vitro* showed decreased osteoclast number after a short-term treatment period. Although serum TRAcP5b was reduced *in vivo* 1 week after a single injection of trabectedin, it was not significantly altered after 6 weeks of trabectedin treatment. Most importantly, histologic analysis of osteoclasts on the trabecular bone surface revealed no significant difference or trend after 1 week or 6 weeks of trabectedin treatment. That trabectedin is capable of directly effecting osteoclasts is not surprising given its already established impact on macrophages. Indeed, osteoclasts are susceptible to TRAIL-mediated apoptosis.^(32,33) However, the *in vivo* analyses of osteoclasts on the bone surface showed no significant change. It may be that that analysis of osteoclast surface at time points closer to the injection of trabectedin (<1 week) would show a difference and align with observed *in vitro* effects. We note that previous analysis of osteoclast on the bone surface in models of macrophage depletion such as the MAFIA (Macrophage Fas-Induced apoptosis) and clodronate models similarly did not show a significant difference.⁽⁴⁾ This may collectively suggest that osteoclasts are a prioritized and conserved differentiation pathway of the myeloid lineage, or have the ability to quickly reconstitute.

The results of this work have immediate clinical relevance to patients currently receiving trabectedin for a variety of sarcomas. In particular, these patients may be at increased risk of fracture on account of reduced bone mass. Moreover, trabectedin is currently being explored for the treatment of breast and prostate cancer,⁽¹⁷⁾ which preferentially metastasize to the skeleton. Given that bone cells have been shown to play a role regulating skeletal metastasis,⁽³⁴⁾ and that trabectedin modulates bone cells and the bone microenvironment, it will be important to consider if potential trabectedin effects on metastasis are due to altering bone cells in addition to directly inhibiting tumor cells.

In this study, we observed that iPTH was effective at increasing trabecular bone mass in trabectedin-treated mice. This data has several implications. First, it may generally suggest that an anabolic strategy may be an effective therapeutic option to increase bone mass in patients receiving trabectedin. Although iPTH is not available for use in cancer patients, other anabolic bone treatments are in clinical trials.⁽³⁵⁾ Prior data suggest that iPTH anabolism may be regulated by macrophages and efferocytosis^(4,36); however, the data presented here suggest that partially inhibiting macrophages and efferocytosis with trabectedin does not inhibit the anabolic actions of PTH. It is possible that inhibiting macrophages and efferocytosis by a greater magnitude may further compromise PTH anabolic effects.

Finally, there are several limitations to this study. First, all experiments were carried out in noncancerous models to assess the effect of macrophages and efferocytosis on bone during normal homeostasis. Thus, the results of this study may not directly model a cancer patient receiving trabectedin. An additional limitation is that experiments in this study were performed in male mice, and therefore results may differ in females. Finally, results focused on the appendicular skeleton, and trabectedin effects may differ in axial skeletal sites.

In summary, this study adds new data regarding the role of macrophages and efferocytosis within the bone microenvironment. Importantly, it suggests that in addition to macrophage number, the efferocytic function of macrophages in the bone microenvironment may also regulate bone homeostasis. In addition, because patients are currently receiving trabectedin but the bone phenotype of trabectedin has not been previously described, the data in this study has immediate clinical relevance.

Disclosures

LCH: Consultancy for Alexion, Amgen, Shire, Lilly, Radius, and UCB to institution and personally; payment for development of educational presentations for Alexion, Amgen, and UCB to institution and personally. All other authors (BPS, LZ, AJK, MNM, JIA, HR, LKM) have no disclosures.

Acknowledgments

This study was supported by the National Institutes of Health DK053904 (LKM) and CA093900 (LKM) and P30AR069620 (Univ. Michigan), DOD W81XWH-14-1-0408 (BPS), NIH F30DE025154 (MNM), and Deutsche Forschungsgemeinschaft Forschergruppe-1586 SKELMET (LCH). We acknowledge Michelle Lynch and Justin Do for μ CT assistance, and Chris Strayhorn for histology sectioning.

Authors' roles: Study design: BPS and LKM. Study conduct: BPS, LZ, MNM, and AJK. Data collection: BPS, LZ, AJK, MN, and JIA. Data analysis: BPS, LZ, and JIA. Data interpretation: All authors. Drafting manuscript: BPS and LKM. Revising and approving manuscript: All authors. BPS and LKM take responsibility for the integrity of the data analysis.

References

- Horwood NJ. Macrophage polarization and bone formation: a review. *Clin Rev Allergy Immunol*. 2016;51(1):79–86.
- Sinder BP, Pettit AR, McCauley LK. Macrophages: their emerging roles in bone. *J Bone Miner Res*. 2015;30(12):2140–9.
- Chang MK, Raggatt L-J, Alexander KA, et al. Osteal tissue macrophages are intercalated throughout human and mouse bone lining tissues and regulate osteoblast function in vitro and in vivo. *J Immunol*. 2008;181(2):1232–44.
- Cho SW, Soki FN, Koh AJ, et al. Osteal macrophages support physiologic skeletal remodeling and anabolic actions of parathyroid hormone in bone. *Proc Natl Acad Sci U S A*. 2014;111(4):1545–50.
- Parfitt AM. Bone-forming cells in clinical conditions. In: Hall B, editor. *Bone*. Vol 1 Osteoblast Osteocyte. Boca Raton, FL: CRC Press; 1990. p. 351–429.
- Jilka RL, Weinstein RS, Bellido T, Parfitt AM, Manolagas SC. Osteoblast programmed cell death (apoptosis): modulation by growth factors and cytokines. *J Bone Miner Res*. 1998;13(5):793–802.
- Medeiros AI, Serezani CH, Lee SP, Peters-Golden M. Efferocytosis impairs pulmonary macrophage and lung antibacterial function via PGE2/EP2 signaling. *J Exp Med*. 2009;206(1):61–8.
- Vandivier RW, Henson PM, Douglas IS. Burying the dead: the impact of failed apoptotic cell removal (efferocytosis) on chronic inflammatory lung disease. *Chest*. 2006;129(6):1673–82.
- Thorp E, Cui D, Schrijvers DM, Kuriakose G, Tabas I. Merck receptor mutation reduces efferocytosis efficiency and promotes apoptotic cell accumulation and plaque necrosis in atherosclerotic lesions of apoE^{-/-} mice. *Arterioscler Thromb Vasc Biol*. 2008;28(8):1421–8.
- Thorp E, Tabas I. Mechanisms and consequences of efferocytosis in advanced atherosclerosis. *J Leukoc Biol*. 2009;86(5):1089–95.
- Shao W-, Cohen PL. Disturbances of apoptotic cell clearance in systemic lupus erythematosus. *Arthritis Res Ther*. 2011;13(1):202.
- Soki FN, Koh AJ, Jones JD, et al. Polarization of prostate cancer-associated macrophages is induced by milk fat globule-EGF factor 8 (MFG-E8)-mediated efferocytosis. *J Biol Chem*. 2014;289(35):24560–72.
- Huynh M-LN, Fadok VA, Henson PM. Phosphatidylserine-dependent ingestion of apoptotic cells promotes TGF-beta1 secretion and the resolution of inflammation. *J Clin Invest*. 2002;109(1):41–50.
- Xiao YQ, Freire-de-Lima CG, Schiemann WP, Bratton DL, Vandivier RW, Henson PM. Transcriptional and translational regulation of TGF- β production in response to apoptotic cells. *J Immunol*. 2008;181(5):3575–85.
- Michalski MN, Koh AJ, Weidner S, Roca H, McCauley LK. Modulation of osteoblastic cell efferocytosis by bone marrow macrophages. *J Cell Biochem*. 2016 Dec;117(12):2697–706.
- Germano G, Frapolli R, Belgiovine C, et al. Role of macrophage targeting in the antitumor activity of trabectedin. *Cancer Cell*. 2013;23(2):249–62.
- ClinicalTrials.gov. Trabectedin studies. Available from: <https://clinicaltrials.gov/ct2/results?term=trabectedin>.
- Bouxsein ML, Boyd SK, Christiansen BA, Guldberg RE, Jepsen KJ, Müller R. Guidelines for assessment of bone microstructure in rodents using micro-computed tomography. *J Bone Miner Res*. 2010;25(7):1468–86.
- Parfitt AM, Drezner MK, Glorieux FH, et al. Bone histomorphometry: standardization of nomenclature, symbols, and units. Report of the ASBMR Histomorphometry Nomenclature Committee. *J Bone Miner Res*. 1987;2(6):595–610.
- Dempster DW, Compston JE, Drezner MK, et al. Standardized nomenclature, symbols, and units for bone histomorphometry: a 2012 update of the report of the ASBMR Histomorphometry Nomenclature Committee. *J Bone Miner Res*. 2013;28(1):2–17.
- Alexander KA, Raggatt L-J, Millard S, et al. Resting and injury-induced inflamed periosteum contain multiple macrophage subsets that are located at sites of bone growth and regeneration. *Immunol Cell Biol*. 2017;95(1):7–16.
- Livak KJ, Schmittgen TD. Analysis of relative gene expression data using real-time quantitative PCR and the 2^{- $\Delta\Delta$ C_T} method. *Methods*. 2001;25(4):402–8.
- Wang D, Christensen K, Chawla K, Xiao G, Krebsbach PH, Franceschi RT. Isolation and characterization of MC3T3-E1 preosteoblast subclones with distinct in vitro and in vivo differentiation/mineralization potential. *J Bone Miner Res*. 1999;14(6):893–903.
- Datta NS, Chen C, Berry JE, McCauley LK. PTHrP signaling targets Cyclin D1 and induces osteoblastic cell growth arrest. *J Bone Miner Res*. 2005;20(6):1051–64.
- Koh AJ, Beecher CA, Rosol TJ, McCauley LK. 3',5'-Cyclic adenosine monophosphate activation in osteoblastic cells: effects on parathyroid hormone-1 receptors and osteoblastic differentiation in vitro. *Endocrinology*. 1999;140(7):3154–62.
- Pettit AR, Chang MK, Hume DA, Raggatt L-J. Osteal macrophages: a new twist on coupling during bone dynamics. *Bone*. 2008;43(6):976–82.

27. Mori G, Brunetti G, Colucci S, et al. Alteration of activity and survival of osteoblasts obtained from human periodontitis patients: role of TRAIL. *J Biol Regul Homeost Agents*. 2007; 21(3–4): 105–14.
28. Tinhofer I, Biedermann R, Krismer M, Crazzolara R, Greil R. A role of TRAIL in killing osteoblasts by myeloma cells. *FASEB J*. 2006;20(6):759–61.
29. Atkins GJ, Bouralexis S, Evdokiou A, et al. Human osteoblasts are resistant to Apo2L/TRAIL-mediated apoptosis. *Bone*. 2002;31(4):448–56.
30. Pereira RC, Delany AM, Canalis E. CCAAT/enhancer binding protein homologous protein (DDIT3) induces osteoblastic cell differentiation. *Endocrinology*. 2004;145(4):1952–60.
31. Shirakawa K, Maeda S, Gotoh T, et al. CCAAT/enhancer-binding protein homologous protein (CHOP) regulates osteoblast differentiation. *Mol Cell Biol*. 2006;26(16):6105–16.
32. Zauli G, Rimondi E, Nicolini V, Melloni E, Celeghini C, Secchiero P. TNF-related apoptosis-inducing ligand (TRAIL) blocks osteoclastic differentiation induced by RANKL plus M-CSF. *Blood*. 2004;104(7):2044–50.
33. Roux S, Lambert-Comeau P, Saint-Pierre C, Lépine M, Sawan B, Parent J-L. Death receptors, Fas and TRAIL receptors, are involved in human osteoclast apoptosis. *Biochem Biophys Res Commun*. 2005;333(1):42–50.
34. Logothetis CJ, Lin S-H. Osteoblasts in prostate cancer metastasis to bone. *Nat Rev Cancer*. 2005;5(1):21–8.
35. McClung MR, Grauer A, Boonen S, et al. Romosozumab in postmenopausal women with low bone mineral density. *N Engl J Med*. 2014;370(5):412–20.
36. McCauley LK, Dalli J, Koh AJ, Chiang N, Serhan CN. Cutting edge: parathyroid hormone facilitates macrophage efferocytosis in bone marrow via proresolving mediators resolvins D1 and resolvins D2. *J Immunol*. 2014;193(1):26–9.